Supplementary Information

RNAi induced hepatotoxicity results from loss of the first synthesized isoform of miR-122 in mice

Paul N. Valdmanis, Shuo Gu, Kirk Chu, Lan Jin, Feijie Zhang, Elizabeth M. Munding, Yue Zhang, Yong Huang, Huban Kutay, Kalpana Ghoshal, Leszek Lisowski, and Mark A. Kay

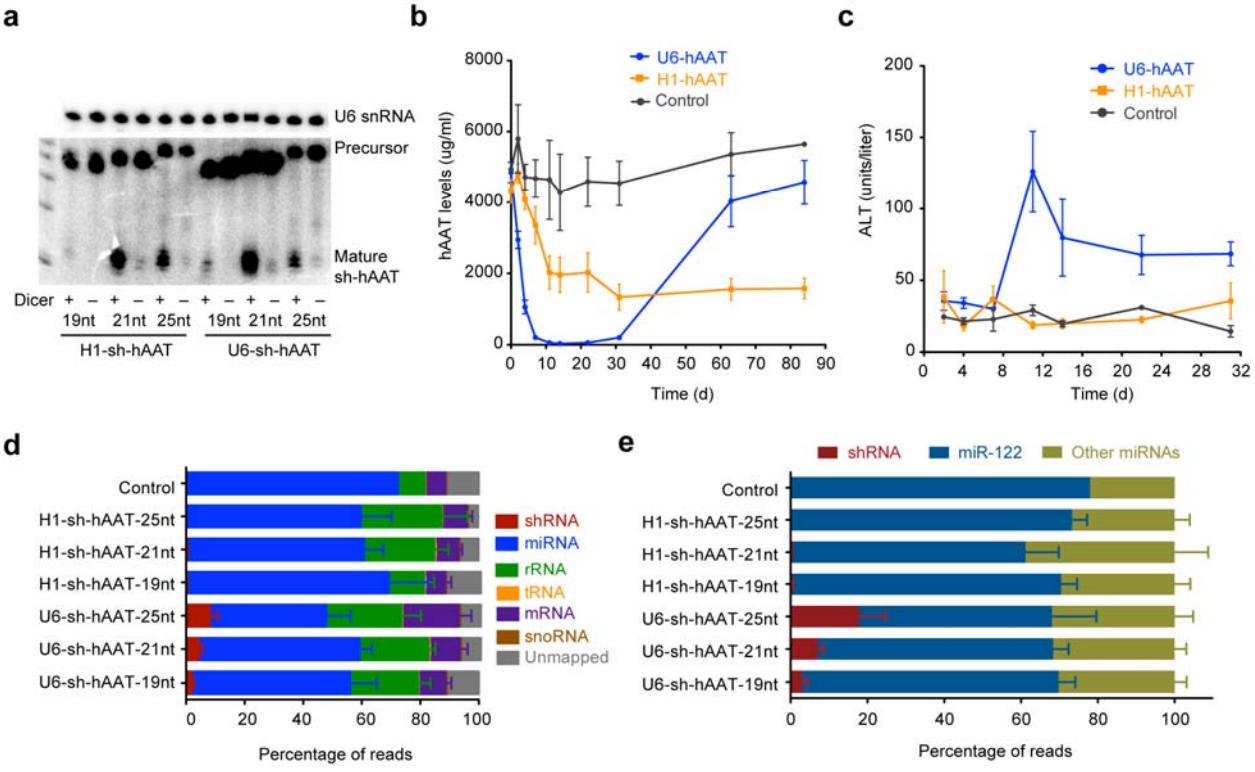

Supplementary Figure 1 shRNA reads specifically compete with miR-122 in Ago2-immunoprecipitated (Ago2-IP) small RNA fractions. (**a**) Mature and precursor hAAT shRNAs of various stem lengths in the presence (+) or absence (–) of Dicer in HEK293 cells. (**b**) hAAT profiles for AAVs expressing all combined U6 or H1 shRNAs compared to control, $n = 9$ mice per treatment except control where $n = 3$; error bars are ± s.e.m. (**c**) ALT levels for each shRNA construct, values and analysis as in (**b**). (**d**) The profile of other small RNAs are unchanged in the Ago2-IP sequenced small RNA fraction; $n = 3$ mice per condition except for control where $n = 1$, error bars are ± s.e.m. (**e**) The proportion of reads mapping to shRNAs similarly compete out miR-122 in Ago2-IP fractions; $n = 3$ mice per condition except for control where $n = 1$, error bars are ± s.e.m.

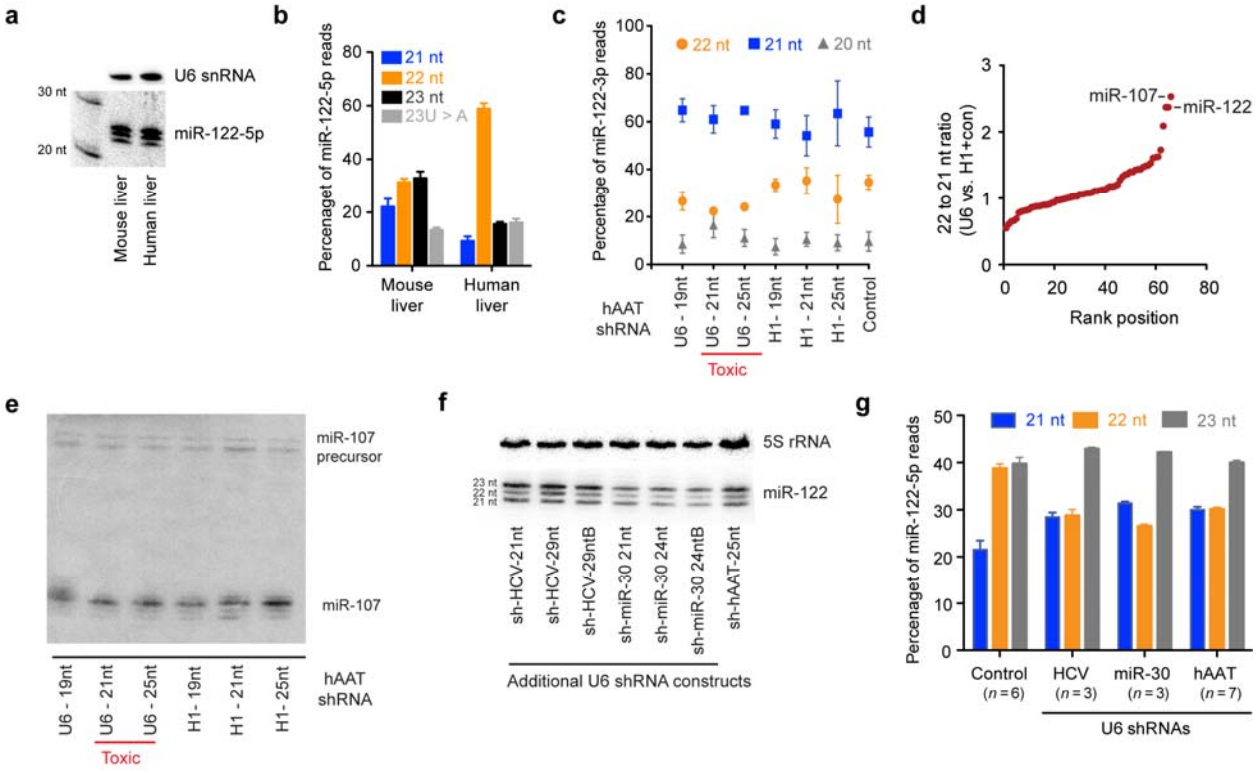

Supplementary Figure 2 Analysis of isoform biogenesis for miR-122 and other microRNAs. (**a**) Isoforms of miR-122-5p are comparable in normal human and mouse liver samples. (**b**) Analysis of deposited small RNA deep sequencing data (GEO submission GSE57381)[1] of human liver samples indicates that the most predominant isoform of miR-122-5p is 22nt in length. Mouse liver controls are from **Fig. 2b**; $n = 4$ for human liver, $n = 3$ for mouse, error bars are ± s.d. (**c**) miR-122-3p reads do not have a change in isoform distribution between toxic U6 samples and non-toxic H1 or controls; $n = 3$ mice per condition, error bars are ± s.e.m. (**d**) Only a few microRNAs (miR-107, miR-22 and miR-19b) have altered 22:21 nucleotide ratios in situations where isoforms of both lengths are expressed. (**e**) Levels of miR-107, another microRNA that show isoform differences based on small RNA sequencing, does not have an obvious isoform difference when tested by small RNA northern. (**f**) Additional shRNA constructs that mimic miR-30 or target the hepatitis C virus (HCV) show the same loss of a 22nt isoform of miR-122. (**g**) Northern blot quantification of the loss of this 22nt species is consistent regardless of the shRNA sequence and its target gene; error bars are ± s.e.m.

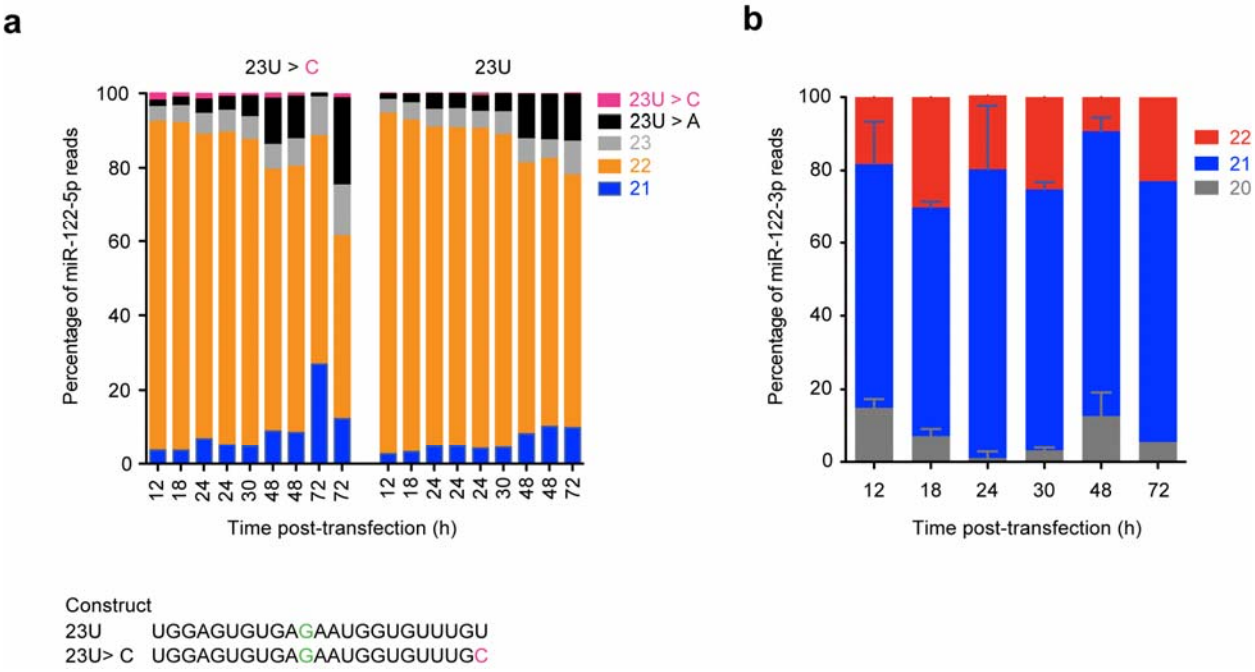

Supplementary Figure 3 The 23rd nucleotide of miR-122-5p is added post-transcriptionally. (**a**) Delivery of pri-miR-122 in HEK293 cells followed by deep sequencing revealed the distribution of isoforms of miR-122. Site directed mutagenesis of the 23rd nucleotide to a cytosine in transfected plasmids (23U > C) still led to addition of a "U" or "A" at this position. Constructs are listed in the bottom panel and include a modified internal residue (green). (**b**) Deep sequencing reads corresponding to miR-122-3p show that all three isoforms (20nt, 21nt and 22nt) are generated at similar levels regardless of the time post-transfection. Replicate numbers are the sum of samples from different time points in (**a**); error bars are ± s.e.m.

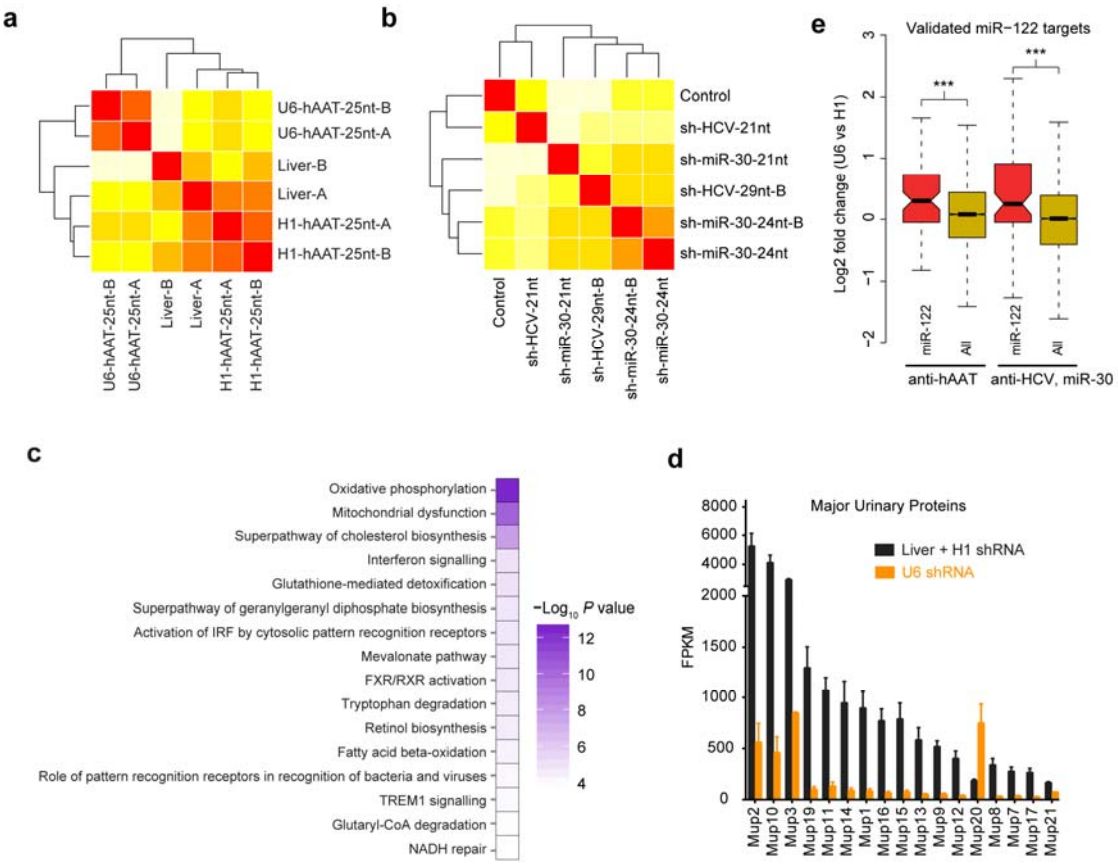

Supplementary Figure 4 RNAseq of shRNA toxic livers reveals concordant dysregulation of mRNA targets. (**a**) Heatmap clustering of liver RNAseq samples by Fragments Per Kilobase of transcript per Million mapped reads (FPKM) values receiving either no shRNA, H1-shRNA or U6-shRNA, $n = 2$ mice per condition (**b**) Heatmap clustering of five additional mice receiving various U6-shRNAs. (**c**) Ingenuity pathway analysis pathways most significantly altered when combining all seven U6-shRNA RNAseq samples relative to five H1-shRNA and controls. (**d**) RNAseq expression reveals a decrease of nearly all major urinary protein (*Mup*) family member expression levels (except for *Mup20*). (**e**) Fold-change expression of FPKM values of validated targets of miR-122 that are de-repressed in livers receiving U6-shRNAs. *** $P < 0.001$ by two-tailed Student's *t* test.

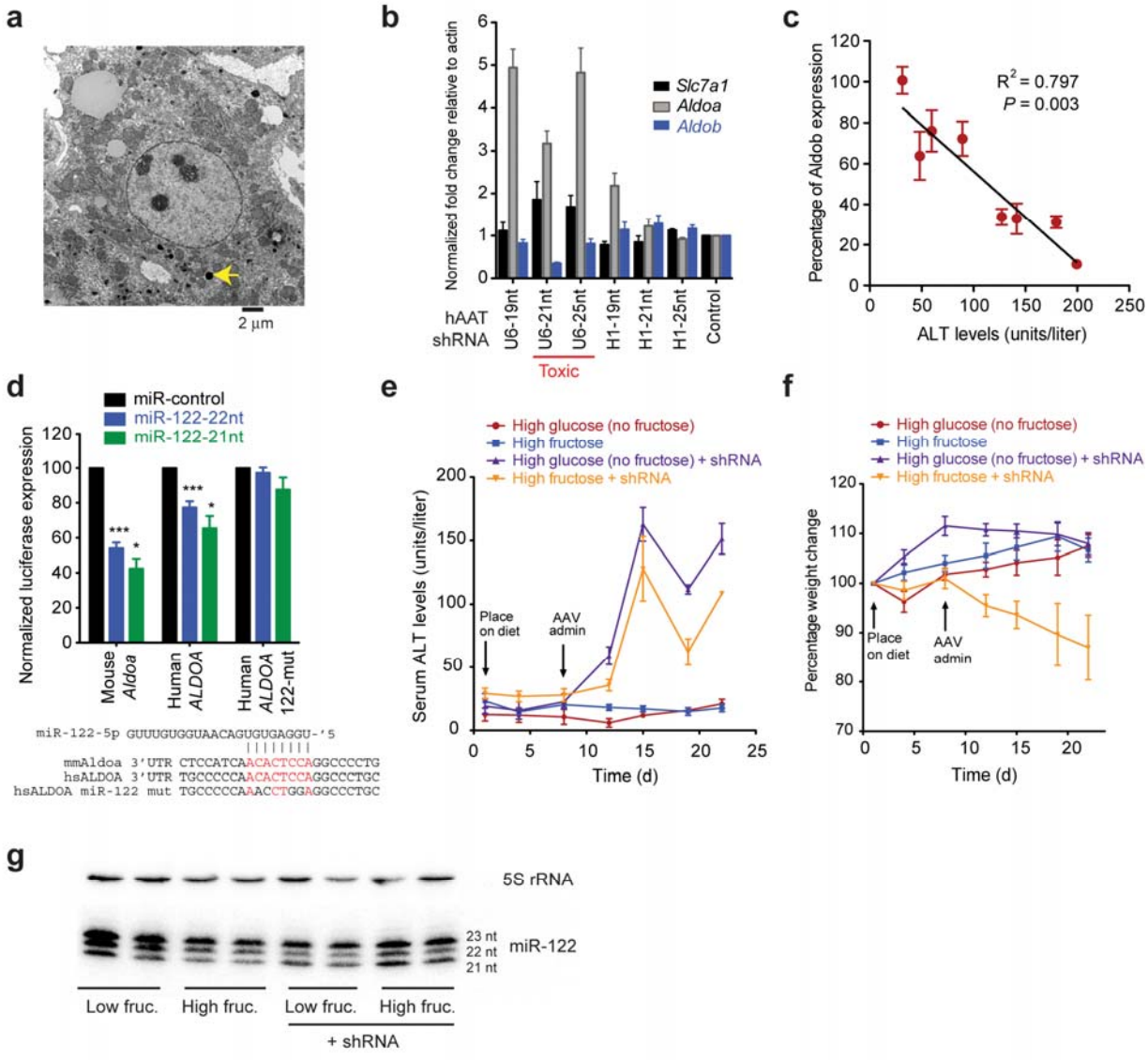

Supplementary Figure 5 Loss of miR-122 leads to functional metabolic consequences including loss of Aldob expression and intolerance to a fructose rich diet. (**a**) Electron micrograph image reveals glycogen rich deposits (arrow) and lipid accumulation in mouse livers receiving shRNAs. (**b**) qPCR analysis reveals that *Aldoa* levels increase in samples with reduced miR-122 levels, with a corresponding decrease in *Aldob* levels, commensurate with an inverse expression pattern of Aldoa and Aldob (and miR-122) in the developing liver[2-4]. *Slc7a1*, another miR-122 target[5] is also de-repressed. (**c**) ALT levels measured in the blood correlate with percent *Aldob* mRNA expression in the liver of seven mice receiving different U6-driven shRNA constructs relative to a control mouse. Data represent 3 independent experiments in triplicate of

one individual mouse per condition; error bars are ± s.e.m. (**d**) Luciferase expression of mouse *Aldoa* and human *ALDOA* 3′UTRs show that a target site is present for miR-122 and site directed mutagenesis of this target releases this repression and both 22nt and 21nt isoforms of miR-122 target this region equally. (**e**) Serum alanine transaminase (ALT) activity showed that diets rich in fructose (60%) and glucose (60% with no fructose) corresponded to increases in ALT levels and liver toxicity; $n = 5$ mice per condition. (**f**) Mouse body weight changes following fructose rich or glucose rich diets and AAV administration revealed a decline in body weight specific to a fructose rich diet; $n = 5$ mice per condition. (**g**) Small RNA northern studies show a decrease in 22nt miR-122 isoforms in samples receiving shRNAs; error bars are ± s.e.m.

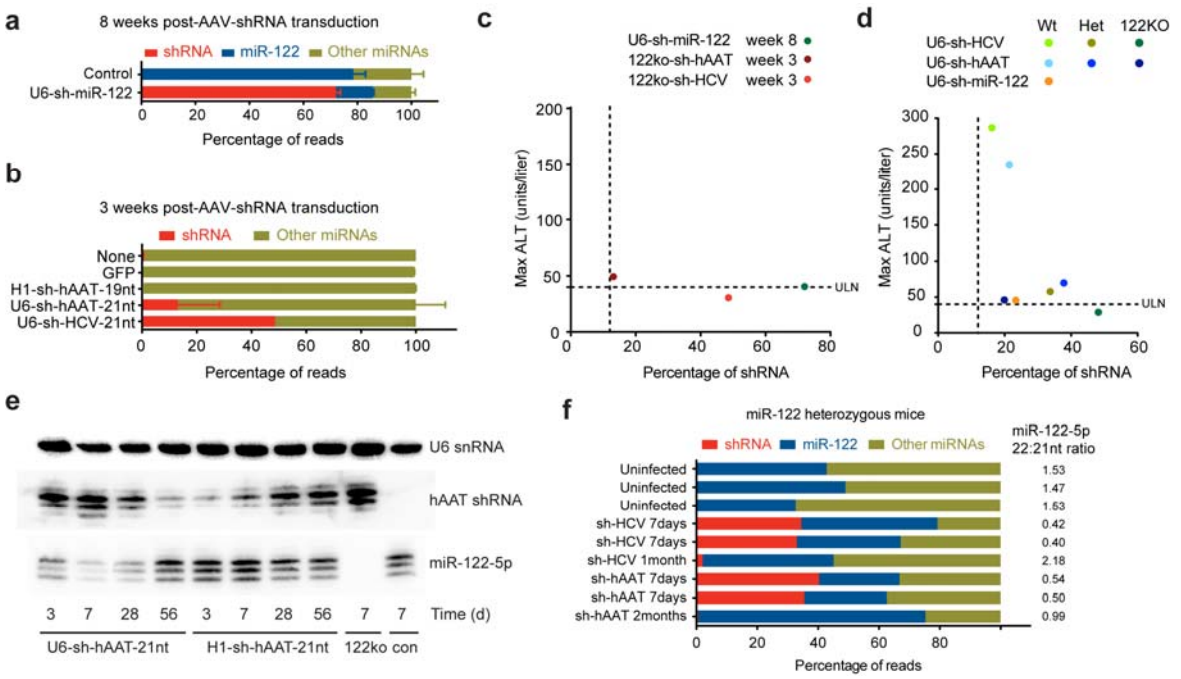

Supplementary Figure 6 Analysis of small RNA sequencing reads derived from shRNAs compared to microRNAs at later time points post-AAV transduction. (**a**) The proportion of reads from U6-sh-miR-122 at week 8 relative to microRNAs. Controls are from **Fig. 1f**, $n = 3$ mice per condition, error bars are ± s.e.m. (**b**) Proportion of reads from shRNAs relative to microRNAs from various AAV vectors in miR-122 knockout mice 3 weeks post-transduction, $n = 2$ mice per condition except for U6-sh-HCV where $n = 1$. (**c**) Percent shRNA relative at indicated times relative to maximum ALT levels measured over 1 month. $N = 3$ mice for U6-sh-miR-122 and 2 for sh-hAAT and sh-HCV. ULN, upper limit normal (**d**) Percent shRNA expression at day 7 relative to maximum ALT levels measured over 1 month. Vertical dashed line indicates the maximum tolerated threshold of 12% in normal mouse livers, horizontal dashed line indicates the upper limit normal of ALT values, $n = 3$ mice for U6-sh-miR-122 and wildtype (wt) U6-sh-hAAT, $n = 2$ for heterozygous (het) mice and $n = 1$ mouse for the remaining samples. U6-hAAT-25nt and U6-HCV in normal liver are included from **Fig. 1d** for comparison purposes; error bars are ± s.e.m. (**e**) Northern blot probing for miR-122 and hAAT small hairpin RNAs in mice at various time points post-AAV-shRNA transduction; 122ko = miR-122 knockout. (**f**) Percent shRNA expression at indicated time points for various rAAV-U6-shRNA constructs in mice heterozygous for miR-122 expression.

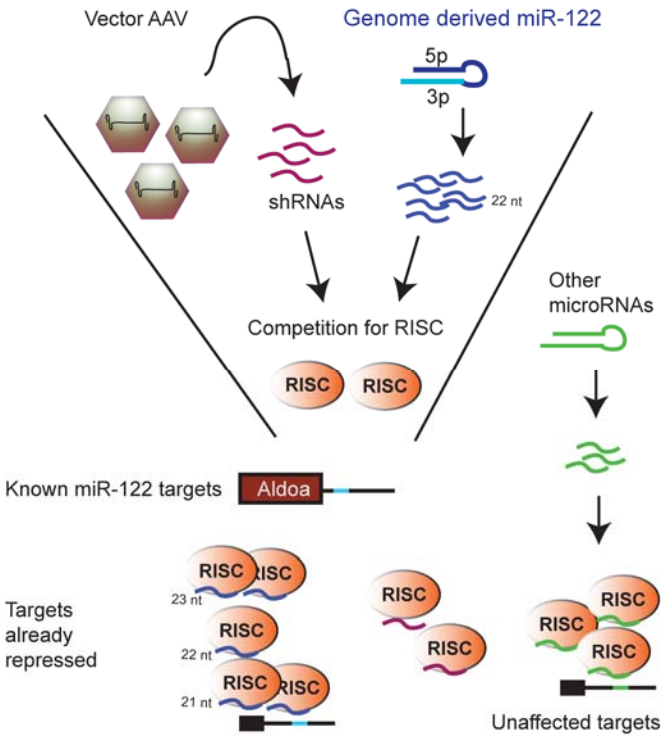

Supplementary Figure 7 Model of proposed mechanism. AAVs expressing shRNAs compete with the first synthesized 22nt isoform of miR-122 for available RISC complexes. This may de-repress newly synthesized mRNAs that would otherwise be targeted by miR-122 leading to liver toxicity. Other microRNAs are largely unaffected in this process.

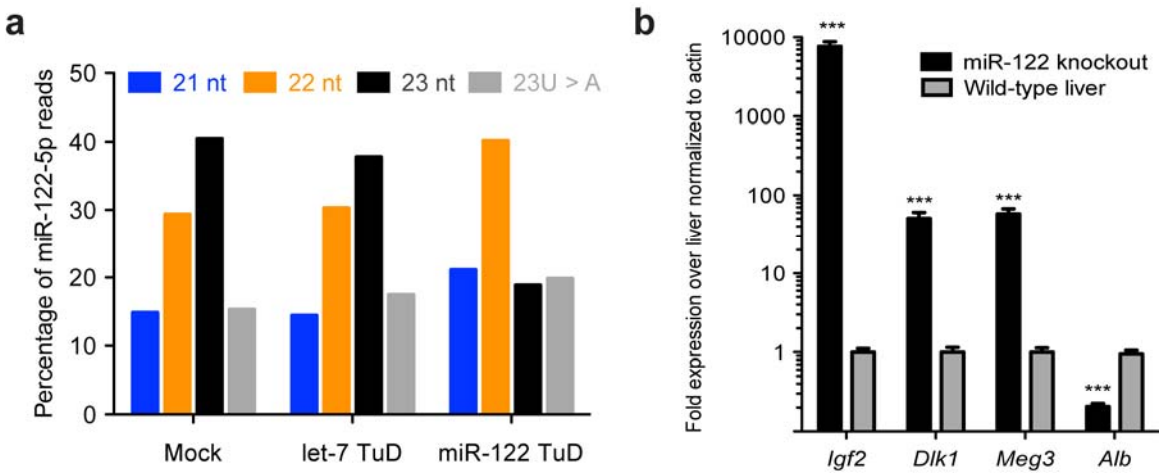

Supplementary Figure 8 miR-122 isoforms after antisense inhibition and mRNA profiles in miR-122 knockout mice (**a**) miR-122-5p isoform proportions in mouse liver after delivery of miR-122 or let-7 "tough decoy" RNAs (TuD). Data is extracted from GEO accession # GSE25971[6]. In each case, reads were counted for the four most abundant miR-122 isoforms and expressed as a relative percentage. miR-122 TuDs specifically diminished the 23nt isoform of miR-122-5p leaving the 22nt isoform relatively unchanged. (**b**) miR-122 knockout mice retain embryonic gene expression profiles. qRT-PCR quantification of mRNA transcripts typically expressed in embryonic but not adult liver, n = 14 mice for miR-122 knockout, n = 11 for control. *** $P < 0.001$ by two-tailed Student's t test.

Supplementary Table 1. Top expressing microRNAs relative to small hairpin RNA read counts.

microRNA	U6 total average	U6 95% CI	H1 total average	H1 total 95% CI	U6 Ago2-IP average	U6 Ago2-IP 95% CI	H1 Ago2-IP average	H1 Ago2-IP 95% CI
miR-122	500852.0	(441459–560245)	648908.8	(553961–743856)	551729.3	(463154–640308)	704482.7	(632652–776312)
shRNA	242568.5	(191761–293376)	5393.8	(672–10115)	167453.9	(89136–245772)	6316.8	(–372–13004)
miR-21	32601.5	(17405–47798)	45797.4	(34306–57288)	31929.3	(16666–47193)	26584.3	(15696–37471)
miR-let-7a-2	18078.5	(14890–21267)	25910.7	(17752–34068)	30547.5	(25743–35352)	32749.4	(18623–46875)
miR-let-7c-2	14387.0	(11329–17445)	16593.6	(11853–21334)	19686.4	(15985–23388)	20017.0	(13250–26783)
miR-let-7f-2	13475.0	(9925–17025)	24615.7	(9703–39528)	15981.2	(11033–20929)	23359.6	(4883–41835)
miR-126	13134.5	(11107–15162)	8502.6	(6880–10124)	6598.8	(4845–8353)	3710.1	(2107–5313)
miR-let-7c-1	12988.0	(10165–15811)	14924.6	(10562–19286)	17332.2	(14010–20654)	18390.6	(12186–24594)
miR-let-7f-1	11038.6	(8199–13878)	20261.2	(8202–32320)	13028.0	(9507–16549)	19069.4	(4383–33755)
miR-let-7b	10477.8	(8609–12346)	14434.4	(9185–19683)	15897.1	(12931–18863)	20364.7	(12941–27787)
miR-let-7d	7666.6	(6784–8549)	10815.5	(7836–13794)	11216.7	(10063–12370)	9877.5	(7079–12675)
mmu-mir-192	7608.3	(5970–9247)	17090.3	(12998–21181)	4747.3	(3120–6374)	11327.1	(6803–15851)
miR-let-7g	7112.7	(5048–9177)	13252.7	(8565–17939)	7818.9	(5536–10102)	8852.5	(6236–11468)
miR-29a	6883.4	(5754–8013)	7819.4	(5743–9895)	5679.6	(4416–6943)	4449.3	(2811–6086)
miR-26b	6479.7	(5249–7711)	10949.0	(5695–16202)	4635.5	(2939–6332)	6409.6	(3310–9509)
miR-143	5699.0	(3354–8043)	2139.7	(1360–2918)	5391.6	(3049–7734)	1596.4	(1004–2188)
miR-142	3948.8	(2748–5150)	1803.6	(1195–2411)	6238.5	(4168–8309)	1718.5	(1430–2007)
miR-22	1543.9	(924–2164)	3806.5	(2299–5313)	3039.7	(779–5300)	2849.2	(1950–3748)

Values are presented as normalized reads per million mapped microRNAs and shRNAs. U6 samples include U6-sh-hAAT-21nt and U6-sh-hAAT-25nt (n = 6); H1 samples include all H1-sh-hAAT samples (n = 9). IP, immunoprecipitated; CI, confidence interval.

Supplementary Table 6. Serum lipid and glucose levels for mice receiving fructose or gluctose rich diets with or without U6-sh-hAAT-25nt shRNAs.

Test	Reference range	Units	low fructose	high fructose	low fructose + U6-shRNA	high fructose + U6-shRNA	Chow + U6-sh-miR-30	Chow + U6-sh-hAAT-	con
Glucose	184–220	mg / dL	181	297	166	71	117	197	213
Cholesterol		mg / dL	102	97	60	44	43	37	84
Triglycerides		mg / dL	64	53	61	23	18	74	61
HDL		mg / dL	104	93	50	30	45	30	79
LDL		mg / dL	10	11	11	28	4	3	9
HDL : LDL			10.4	8.5	4.5	1.1	11.3	10	8.8
BUN	20.3–24.7	mg / dL	24	28	20	23	12	19	25
Creatinine	0.1–1.1	mg / dL	0.1	0.4	0.3	0.2	0.2	0.1	0.3
Total Protein	5.0–6.2	g / dL	5.2	5.2	4.5	3.3	4.1	4.1	4.8

HDL, high-density lipoprotein; LDL, low-density lipoprotein; BUN, blood urea nitrogen; con, control.

Supplementary Table 7. List of primers used for shRNA cloning, luciferase cloning and small RNA sequence alignment.

sh-hAAT-19nt-S	CACCGAAGCGTTTAGGCATGTTTTCAAGAGAAACATGCCTAAACGCTTC
sh-hAAT-19nt-A	AAAAGAAGCGTTTAGGCATGTTTCTCTTGAAAACATGCCTAAACGCTTC
sh-hAAT-21nt-S	CACCGAAGCGTTTAGGCATGTTTAATCAAGAGTTAAACATGCCTAAACGCTTC
sh-hAAT-21nt-A	AAAAGAAGCGTTTAGGCATGTTTAACTCTTGATTAAACATGCCTAAACGCTTC
sh-hAAT-25nt-S	CACCGAAGCGTTTAGGCATGTTTAACATCTCAAGAGGATGTTAAACATGCCTAAACGCTTC
sh-hAAT-25nt-A	AAAAGAAGCGTTTAGGCATGTTTAACATCCTCTTGAGATGTTAAACATGCCTAAACGCTTC
sh-miR-122-S	CACCGAACGCCATTATCACACTCTATACCTGACCCATATGGAGTGTGAGAATGGTGTTTTTTGTAC
sh-miR-122-A	AAAAACACCATTCTCACACTCCATATGGGTCAGGTATAGAGTGTGATAATGGCGTTC
sh-HCV-21-S	GATCGACTTATCCAGTTGGTTCACTCCTGACCCAAGTGAACCAACTGGATAAGTCTTTTTGTAC
sh-HCV-21-A	AAAAGACTTATCCAGTTGGTTCACTTGGGTCAGGAGTGAACCAACTGGATAAGTC
sh-HCV-29-S	GATCCACCGACTTATCCAGTTGGTTCACTGATGCTACCCTGACCCAGTAGCATCAGTGAACCAACTGGATAAGTCTTTTTGTAC
sh-HCV-29-A	AAAAGACTTATCCAGTTGGTTCACTGATGCTACTGGGTCAGGGTAGCATCAGTGAACCAACTGGATAAGTC
sh-HCV-29B-S	GATCCACCGACTTATCCAGTTGGTTCACTCCTGCTACCCTGACCCAGTAGCCCAAGTGAACCAACTGGATAAGTCTTTTTGTAC
sh-HCV-29B-A	AAAAGACTTATCCAGTTGGTTCACTTGGGCTACTGGGTCAGGGTAGCAGGAGTGAACCAACTGGATAAGTC
sh-miR-30-21-S	GATCCACCGCTGCAAACATCCGACTGAACCCTGACCCAGTTCAGTCGGATGTTTGCAGCTTTTTGTAC
sh-miR-30-21-A	AAAAGCTGCAAACATCCGACTGAACTGGGTCAGGGTTCAGTCGGATGTTTGCAGC
sh-miR-30-24-S	GATCCACCGCTGCAAACATCCGACTGAAAGCTCCTGACCCAAGCTTTCAGTCGGATGTTTGCAGCTTTTTGTAC
sh-miR-30-24-A	AAAAGCTGCAAACATCCGACTGAAAGCTTGGGTCAGGAGCTTTCAGTCGGATGTTTGCAGC
sh- miR-30-24B-S	GATCCACCGCTGCAAACATGCGACTGAAAGCTCCTGACCCAAGCTTTCAGTCGGATGTTTGCAGCTTTTTGTAC

sh-miR-30-24B-A	AAAAGCTGCAAACATCCGACTGAAAGCTTGGGTCAGGAGC TTTCAGTCGCATGTTTGCAGC
hsALDOA UTRpsiF	CTCGAGGCGGAGGTGTTCCCAGGCTGCCCCCAACACTCCA GGCCCTGCCCCCTCCCACTCTTGAAGA
hsALDOA UTRpsiR	ACTAGTCTTCAAGAGTGGGAGGGGGCAGGGCCTGGAGTGT TGGGGGCAGCCTGGGAACACCTCCGCC
hsALDOA UTRmutF	CTCGAGGCGGAGGTGTTCCCAGGCTGCCCCCAAACCTGGA GGCCCTGCCCCCTCCCACTCTTGAAGA
hsALDOA UTRmutR	ACTAGTCTTCAAGAGTGGGAGGGGGCAGGGCCTCCAGGTT TGGGGGCAGCCTGGGAACACCTCCGCC
mmAldoa UTRpsiF	CTCGAGCCAGAGCTGAACTAAGGCTGCTCCATCAACACTC CAGGCCCCTGCCTACCCACTTGCTATA
mmAldoa UTRpsiR	ACTAGTATAGCAAGTGGGTAGGCAGGGGCCTGGAGTGTTG ATGGAGCAGCCTTAGTTCAGCTCTGGC

5′ to 3′ direction for each; S = sense, A = antisense. Mismatches in the miR-122 binding site of human *ALDOA* are underlined,

SUPPLEMENTARY REFERENCES

1. Selitsky, S.R., *et al.* Small tRNA-derived RNAs are increased and more abundant than microRNAs in chronic hepatitis B and C. *Scientific reports* **5**, 7675 (2015).
2. Chang, J., *et al.* miR-122, a mammalian liver-specific microRNA, is processed from hcr mRNA and may downregulate the high affinity cationic amino acid transporter CAT-1. *RNA biology* **1**, 106-113 (2004).
3. Hommes, F.A. & Draisma, M.I. The development of L- and M-type aldolases in rat liver. *Biochim Biophys Acta* **222**, 251-252 (1970).
4. Numazaki, M., Tsutsumi, K., Tsutsumi, R. & Ishikawa, K. Expression of aldolase isozyme mRNAs in fetal rat liver. *European journal of biochemistry / FEBS* **142**, 165-170 (1984).
5. Bhattacharyya, S.N., Habermacher, R., Martine, U., Closs, E.I. & Filipowicz, W. Relief of microRNA-mediated translational repression in human cells subjected to stress. *Cell* **125**, 1111-1124 (2006).
6. Xie, J., *et al.* Long-term, efficient inhibition of microRNA function in mice using rAAV vectors. *Nature methods* **9**, 403-409 (2012).